

See discussions, stats, and author profiles for this publication at: <https://www.researchgate.net/publication/275363296>

Metabonomics Reveals Metabolite Changes in Biliary Atresia Infants

ARTICLE *in* JOURNAL OF PROTEOME RESEARCH · APRIL 2015

Impact Factor: 4.25 · DOI: 10.1021/acs.jproteome.5b00125 · Source: PubMed

CITATION

1

READS

26

16 AUTHORS, INCLUDING:



Kejun Zhou

Xin Hua Hospital Affiliated to Shanghai Jiao...

16 PUBLICATIONS 143 CITATIONS

SEE PROFILE



Guoxiang Xie

University of Hawai'i at Mānoa

75 PUBLICATIONS 1,217 CITATIONS

SEE PROFILE



Yongtao Xiao

Shanghai Jiao Tong University

25 PUBLICATIONS 260 CITATIONS

SEE PROFILE



Wei Jia

University of Hawai'i at Mānoa

262 PUBLICATIONS 6,108 CITATIONS

SEE PROFILE

Metabonomics Reveals Metabolite Changes in Biliary Atresia Infants

Kejun Zhou,^{†,‡} Guoxiang Xie,^{§,||} Jun Wang,[†] Aihua Zhao,[§] Jiajian Liu,[§] Mingming Su,^{||} Yan Ni,^{||} Ying Zhou,[†] Weihua Pan,[†] Yanran Che,[⊥] Ting Zhang,[⊥] Yongtao Xiao,[‡] Yang Wang,[‡] Jie Wen,[‡] Wei Jia,^{*,§,||} and Wei Cai^{*,†,‡}

[†]Department of Pediatric Surgery, Xin Hua Hospital, School of Medicine, Shanghai Jiao Tong University (SJTU), 1665 Kongjiang Road, Shanghai 200092, China

[‡]Shanghai Key Laboratory of Pediatric Gastroenterology and Nutrition, Shanghai Institute for Pediatric Research, 1665 Kongjiang Road, Shanghai 200092, China

[§]Center for Translational Medicine, Six People's Hospital, SJTU School of Medicine, 600 Yishan Road, Shanghai 200230, China

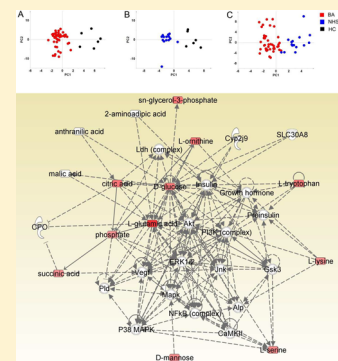
^{||}University of Hawaii Cancer Center, 701 Ilalo Street, Honolulu, Hawaii 96813, United States

[⊥]Department of Infection and Gastroenterology, Shanghai Children's Hospital, SJTU School of Medicine, 1400 West Beijing Road, Shanghai 200040, China

Supporting Information

ABSTRACT: Biliary atresia (BA) is a rare neonatal cholestatic disorder caused by obstruction of extra- and intra-hepatic bile ducts. If untreated, progressive liver cirrhosis will lead to death within 2 years. Early diagnosis and operation improve the outcome significantly. Infants with neonatal hepatitis syndrome (NHS) present similar symptoms, confounding the early diagnosis of BA. The lack of noninvasive diagnostic methods to differentiate BA from NHS greatly delays the surgery of BA infants, thus deteriorating the outcome. Here we performed a metabolomics study in plasma of BA, NHS, and healthy infants using gas chromatography–time-of-flight mass spectrometry. Scores plots of orthogonal partial least-squares discriminant analysis clearly separated BA from NHS and healthy infants. Eighteen metabolites were found to be differentially expressed between BA and NHS, among which seven (L-glutamic acid, L-ornithine, L-isoleucine, L-lysine, L-valine, L-tryptophan, and L-serine) were amino acids. The altered amino acids were quantitatively verified using ultraperformance liquid chromatography–tandem mass spectrometry. Ingenuity pathway analysis revealed the network of “Cellular Function and Maintenance, Hepatic System Development and Function, Neurological Disease” was altered most significantly. This study suggests that plasma metabolic profiling has great potential in differentiating BA from NHS, and amino acid metabolism is significantly different between the two diseases.

KEYWORDS: biliary atresia, neonatal hepatitis syndrome, metabonomics, amino acid



INTRODUCTION

Biliary atresia (BA) is the most common cause of chronic cholestasis in neonates which derived from a fibroinflammatory destruction of extra- or intra-hepatic bile ducts.^{1,2} The incidence ranges from 1 in 5000 to 1 in 20 000 living births in different areas of the world. It constitutes nearly one-third of all neonatal cholestasis or >90% obstructive cholestatic cases.³ If untreated, children will die by age 2 years because of progressive liver cirrhosis.

Neonatal hepatitis syndrome (NHS) is another leading cause of neonatal cholestasis, and there is great overlap in the clinical, biochemical, imaging, and histopathological characteristics between NHS and BA.^{3–5} BA should be differentiated from NHS as soon as possible because early Kasai operations greatly improve the outcome of BA infants, while NHS infants do not need surgery, most of which will usually return to normal by 1 year of age; however, discrimination of BA from NHS is challenging due to the lack of noninvasive diagnostic methods. Currently, clinical determination of BA in an infant with

cholestasis usually requires liver biopsy or operative cholangiography. Patients may undergo a wide range of tests before BA or an alternative diagnosis is reached, which delays the time of Kasai operation in BA patients.

Recently, great effort has been made to search for new BA biomarkers. Some serum metabolites or proteins, including hyaluronic acid,⁶ apolipoprotein C3 (APOC3),⁷ and interleukin 6 (IL-6) and IL-8,⁸ are reported altered in BA. Circulating levels of the miR-200b/429 cluster were found to be elevated in BA infants compared with cholestatic controls;⁹ however, no noninvasive biomarker for BA has been discovered so far. Thus, there is an urgent need for blood biomarkers for BA.

Metabonomics studies the comprehensive small-molecular-weight metabolites and their dynamic changes in biological systems. Mass-spectrometry-based metabolic profiling is increasingly used to uncover new biomarkers for diagnosis,^{10,11}

Received: February 8, 2015

prognosis,^{12,13} and pathogenesis clarification¹⁴ and as potential therapeutic targets for clinical treatment;¹⁵ however, no comprehensive metabolic profiling of BA was reported yet. In this study, we conducted a metabolomics study of 45 BA, 15 NHS, and 6 healthy infants using gas chromatography–time-of-flight-mass spectrometry (GC–TOFMS) to discover the different plasma metabolic compositions. Then, differentially expressed metabolites were verified in plasma of 53 BA and 28 NHS infants using a targeted metabolomics method with ultraperformance liquid chromatography–tandem mass spectrometry (UPLC–MS/MS).

MATERIALS AND METHODS

Chemicals and Reagents

HPLC-grade acetonitrile, methanol, and formic acid were purchased from Merck Chemicals (Darmstadt, Germany). Chloroform, pyridine, anhydrous sodium sulfate, BSTFA (1% TMCS), heptadecanoic acid, methoxyamine, and L-2-chlorophenylalanine were purchased from Sigma-Aldrich (St. Louis, MO). Absolute IDQ P180 kit was purchased from Biocrates Life Sciences (Innsbruck, AT) for targeted quantification of amino acids and biogenic amines.

Clinical Samples

Plasma samples were obtained from 45 BA (before operative cholangiography), 15 NHS, and 6 healthy infants for GC–TOFMS analysis at Xin Hua Hospital, Shanghai, China, from July 2011 to July 2013. Additional 8 BA (before operative cholangiography) and 13 NHS plasma samples were collected from August 2013 to May 2014 in the same hospital. Combined with former samples, a total of 53 BA and 28 NHS was used for validation of amino acids expression. All infants with BA were correctly identified based on operative cholangiography and liver pathology. Cholestasis induced by citrin deficiency, α 1-antitrypsin deficiency, Alagille's syndrome, progressive familial intrahepatic cholestasis, parenteral nutrition, and choledochal cysts was excluded in this study. Plasma samples were kept at -80°C until analysis. Parental consent was provided for all patients to participate in the study. Human sample collection and study protocols were performed in accordance with the guidelines of Xin Hua hospital. All of the experimental protocols were approved by the ethics committee of Xin Hua hospital.

Plasma Sample Preparation and Analysis by GC–TOFMS

Plasma metabolites were first analyzed by GC–TOFMS following our previously published procedure with minor modifications.^{10,16} A 50 μL aliquot of plasma sample was spiked with two internal standard solutions (10 μL of L-2-chlorophenylalanine in water, 0.3 mg/mL; 10 μL of heptadecanoic acid in methanol, 1 mg/mL) and vortexed for 10 s. The mixed solution was extracted with 150 μL of methanol/chloroform (3:1) and vortexed for 30 s. After storing for 10 min at -20°C , the samples were centrifuged at 12 000g for 10 min. An aliquot of the 150 μL supernatant was transferred to a glass sampling vial to vacuum-dry at room temperature. Then, a two-step procedure was used for residue derivatization. First, 50 μL of methoxyamine (15 mg/mL in pyridine) was added to the vial and kept at 30°C for 90 min, followed by 50 μL of BSTFA (1% TMCS) at 70°C for 60 min.

Each 1 μL of aliquot of the derivatized solution was injected into an Agilent 6890N gas chromatography coupled to a Pegasus HT time-of-flight mass spectrometer (Leco Corpo-

ration, St. Joseph, MI) in splitless mode. Metabolites separation was achieved on a DB-5MS capillary column (30 m \times 250 μm I.D., 0.25- μm film thickness; (5%-phenyl)-methylpolysiloxane bonded and cross-linked; Agilent J&W Scientific, Folsom, CA). Helium carrier gas was used at a constant flow rate of 1.0 mL/min. The temperature of injection, transfer interface, and ion source was set to 270, 260, and 200°C , respectively. The GC temperature programming was set to 2 min of isothermal heating at 80°C , followed by $10^{\circ}\text{C}/\text{min}$ oven temperature ramps to 180°C , $5^{\circ}\text{C}/\text{min}$ to 240°C , and $25^{\circ}\text{C}/\text{min}$ to 290°C and a final 9 min maintenance at 290°C . MS measurements were implemented with electron impact ionization (70 eV) in the full-scan mode (m/z 30–600), and the acquisition rate was 20 spectrum/second in the TOFMS setting.

GC–TOFMS Data Analysis

The acquired MS files from GC–TOFMS analysis were processed by ChromaTOF software (v4.50.8.0, Leco, CA). After the pretreatment of baseline correction, denoising, smoothing, alignment, and deconvolution, raw data containing retention time, intensity, and the mass-to-charge ratio of each peak were obtained. Compounds were identified by comparison with the internal library built with the standard reference compounds and NIST 05 standard mass spectral databases software in NIST MS search 2.0 (NIST, Gaithersburg, MD). In brief, GC–TOFMS metabolites were identified by comparing the mass fragments with NIST 05 standard mass spectral databases in NIST MS search 2.0 (NIST, Gaithersburg, MD) software with a similarity of $>70\%$ and finally verified by available reference compounds (in-house library containing ~ 1000 mammalian metabolites). Both mass-spectrum and retention times were used to achieve precise compound annotations. Internal standards and any known artificial peaks, such as peaks caused by noise, column bleed, and BSTFA derivatization procedure, were removed from the data set. Multivariate statistical model of orthogonal partial least-squares discriminate analysis (OPLS-DA) was constructed with the software SIMCA-P+ (version 13.0, Umetrics, Umea, Sweden). On the basis of a variable importance in the projection (VIP) threshold of 1, a number of metabolites responsible for the difference in the metabolic profiles of different groups could be obtained. In parallel, the metabolites identified by the OPLS-DA model were validated at a univariate level using the nonparametric Mann–Whitney U test (SPSS 21) with the critical p value set to 0.05.

Molecular Pathway and Network Analysis in Ingenuity Pathway Analysis (IPA)

To systematically understand the metabolism difference between BA and NHS, we uploaded the metabolite lists (with HMDB IDs) and the change folds of the differentially expressed metabolites onto an IPA server.¹⁷ Canonical pathways and chemical–protein interaction networks were generated based on the knowledge sorted in the Ingenuity Pathway Knowledge base. A ratio of the number of metabolites that map to the canonical pathway divided by the total number of molecules that map to the pathway was displayed. Fisher's exact test was used to calculate a p value determining the probability that the association between the metabolites and the canonical pathway was explained by chance alone. The network score was based on the hypergeometric distribution and was calculated with the right-tailed Fisher's exact test. The higher a score was, the more relevant the eligible submitted molecules were to the network.

Table 1. Demographic and Clinical Investigations of the Sample Set^a

	BA (n = 53)	NHS (n = 28)	HC (n = 6)	p value		
				BA vs HC	NHS vs HC	BA vs NHS
age (days)	67 (32–145)	63 (33–194)	46.5 (29–113)	0.135	0.392	0.111
gender (F/M)	16/37	9/19	2/4	0.874	0.890	0.856
total bilirubin (μmol/L)	156(80–271)	147 (43–419)	4.7 (4–14)	0.000	0.000	0.727
direct bilirubin (μmol/L)	113 (51–181)	99 (32–283)	1.6 (1–6)	0.000	0.000	0.109
total bile acids (μmol/L)	117(34–282)	107 (24–320)	5.6 (3–11)	0.000	0.000	0.798
alanine aminotransferase (U/L)	126 (58–742)	111 (31–427)	25 (7–53)	0.000	0.000	0.153
aspartate aminotransferase (U/L)	231 (81–1440)	176 (61–651)	28 (9–59)	0.000	0.000	0.096
γ-glutamyl transferase (U/L)	670 (123–2074)	186 (41–815)	NA	NA	NA	0.001

^aBA, biliary atresia; NHS, neonatal hepatitis syndrome; HC, healthy control.

Validation of Deferential Amino Acid Metabolism between BA and NHS

A P180 absolute IDQ kit was used to validate the amino acid expressions in plasma of 53 BA and 28 NHS infants. Forty amino acids and biogenic amines were quantitatively measured according to manufacturer's instruction with minor modifications using an ACQUITY ultra-performance liquid chromatography (BEH C18 1.7 μm 2.1 × 100 mm column) coupled to Waters Xevo TQ-S triple quadrupole mass spectrometry. In brief, 10 μL of the internal standard solutions was added to all wells of the plate. Then, 10 μL of plasma or calibration standards was pipetted onto the center of each spot, and samples were dried at room temperature under a stream of nitrogen. 50 μL of freshly prepared 5% v/v phenylisothiocyanate solution was immediately added to each dried well. After 20 min for derivatization, the plate was dried in the nitrogen evaporator for 60 min. 300 μL of extraction solvent (5 mM ammonium acetate in methanol) was added to each well and incubated for 30 min. An aliquot of 5 μL of the derivatized amino acids and biogenic amines was injected for analysis.

RESULTS

Demographic Information and Clinical Manifestations

Demographic and clinical parameters including age, gender, total bilirubin, direct bilirubin, total bile acids, alanine aminotransferase, aspartate aminotransferase, and γ-glutamyl-transferase (GGT) are listed in Table 1. Age and gender showed no significant difference among all of the groups. Both BA and NHS infants have significantly elevated levels of total bilirubin, direct bilirubin, total bile acids, alanine aminotransferase, and aspartate aminotransferase compared with healthy infants because of the severe liver damage of BA and NHS infants; however, these liver function parameters showed no significant difference between BA and NHS, except for GGT ($p = 0.001$).

Plasma Metabonomic Profiling of BA, NHS, and Healthy Infants (HC)

Plasma samples from 45 BA, 15 NHS, and 6 HC infants were conducted to GC–TOFMS metabonomic profiling. After data processing, OPLS-DA was performed on the data set including 78 identified compounds (Table S1 in the SI). Distinct metabolic profiles could be observed from OPLS-DA scores plots between BA and HC (Figure 1A, $R^2X = 0.336$, $R^2Y = 0.803$, $Q^2Y = 0.405$), between NHS and HC (Figure 1B, $R^2X = 0.346$, $R^2Y = 0.868$, $Q^2Y = 0.542$), and between BA and NHS (Figure 1C, $R^2X = 0.316$, $R^2Y = 0.758$, $Q^2Y = 0.389$). On the basis of $VIP > 1$ of the OPLS-DA model and $p < 0.05$ of

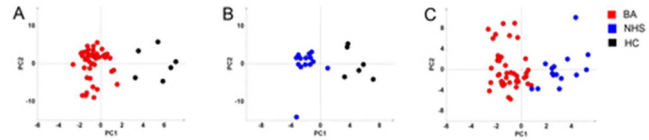


Figure 1. OPLS-DA score plots of metabolic profiles derived from the data of GC–TOFMS among BA, NHS, and HC groups. (A) OPLS-DA score plots between BA and HC. $R^2X = 0.336$, $R^2Y = 0.803$, $Q^2Y = 0.405$. (B) OPLS-DA score plots between NHS and HC. $R^2X = 0.346$, $R^2Y = 0.868$, $Q^2Y = 0.542$. (C) OPLS-DA score plots between BA and NHS. $R^2X = 0.316$, $R^2Y = 0.758$, $Q^2Y = 0.389$.

nonparametric Mann–Whitney U test, a total of 18 metabolites (L-glutamic acid, L-ornithine, L-isoleucine, 2-hydroxy-3-methylbutyric acid, L-lysine, L-valine, D-mannose, L-tryptophan, gluconolactone, L-serine, phosphate, succinic acid, glycerol 3-phosphate, D-glucose, citric acid, oxalic acid, ribitol, and pentanoic acid) were differentially expressed between BA and NHS (Table 2). There were seven amino acids (L-glutamic acid, L-ornithine, L-isoleucine, L-lysine, L-valine, L-tryptophan, and L-serine) among these metabolites.

Table 2. Differentially Expressed Plasma Metabolites between BA and NHS^a

metabolites	VIP	p	ratio (BA/NHS)
L-glutamic acid	2.24	0.000	2.15
L-ornithine	1.26	0.002	1.51
L-isoleucine	1.85	0.005	1.33
2-hydroxy-3-methylbutyric acid	2.01	0.006	0.57
L-lysine	1.74	0.006	1.17
L-valine	1.72	0.007	1.29
D-mannose	1.55	0.008	1.19
L-tryptophan	1.53	0.008	1.44
gluconolactone	1.28	0.023	1.42
L-serine	1.52	0.024	1.24
phosphate	1.26	0.024	1.12
succinic acid	1.17	0.024	1.14
glycerol 3-phosphate	1.11	0.024	1.47
D-glucose	1.33	0.032	1.42
citric acid	1.24	0.034	1.45
oxalic acid	1.88	0.035	0.82
ribitol	1.39	0.035	0.75
pentanoic acid	1.33	0.042	1.42

^aBA, biliary atresia; NHS, neonatal hepatitis syndrome.

IPA Analysis of the Differentially Expressed Metabolites between BA and NHS

The total 18 differentially expressed metabolites were uploaded to IPA Web site for pathway and network analysis. The most significantly altered network was “Cellular Function and Maintenance, Hepatic System Development and Function, Neurological Disease”, with a score of 28 (Figure 2). The five

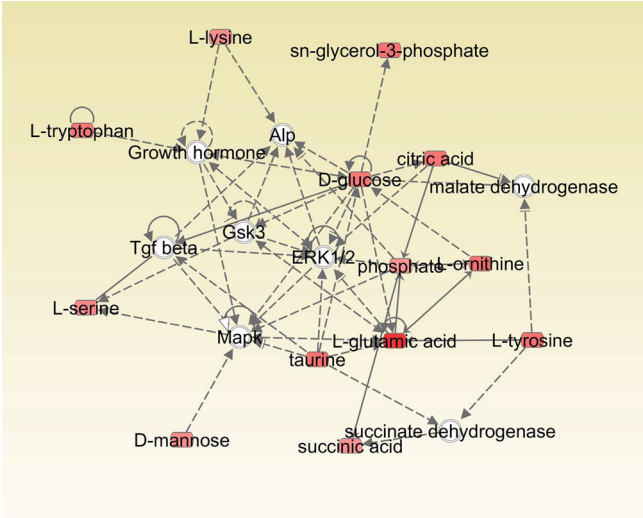


Figure 2. Most significantly differential network between BA and NHS. The network of “Cellular Function and Maintenance, Hepatic System Development and Function, Neurological Disease” was the most significantly altered network between BA and NHS, with a score of 28 and 11 altered metabolites involved. Red means the elevated metabolites in BA compared with NHS.

most significantly different pathways were tRNA charging, serine biosynthesis, glucose and glucose-1-phosphate degradation, proline biosynthesis II (from arginine), and TCA cycle II (Table 3). A total of 11 metabolites (L-glutamic acid, L-

Table 3. Five Most Significantly Altered Canonical Pathways between BA and NHS Revealed by IPA Analysis

canonical pathways	<i>p</i>	differentially expressed metabolites
tRNA charging	2.3×10^{-7}	L-glutamic acid, L-isoleucine, L-lysine, L-serine, L-tryptophan, L-valine
serine biosynthesis	1.2×10^{-4}	L-glutamic acid, L-serine, phosphate
glucose and glucose-1-phosphate degradation	3.1×10^{-4}	D-glucose, gluconolactone, phosphate
proline biosynthesis II (from arginine)	4.0×10^{-4}	L-glutamic acid, L-ornithine, phosphate
TCA cycle II	1.1×10^{-3}	citric acid, phosphate, succinic acid

ornithine, L-lysine, D-mannose, L-tryptophan, L-serine, phosphate, succinic acid, glycerol 3-phosphate, D-glucose, and citric acid) were involved in the network. The amino acids, L-glutamic acid, L-isoleucine, L-lysine, L-serine, L-tryptophan, and L-valine, involved in the tRNA charging were altered most significantly ($p = 2.3 \times 10^{-7}$).

Validation of Amino Acid Metabolism in BA and NHS Infants

To further validate the amino acid expressions in BA and NHS, a total of 40 amino acids and biogenic amines were quantitatively measured using a P180 Absolute IDQ kit in 53

BA and 28 NHS infants. Among these 40 compounds, a total of 34 compounds were quantitatively detected. All seven differentially expressed amino acids (L-glutamic acid, L-ornithine, L-isoleucine, L-lysine, L-valine, L-tryptophan, and L-serine) found by GC-TOFMS were significantly different between BA and NHS in the larger sample set (Figure 3). We also found that taurine was increased in BA compared with NHS infants (Figure 3).

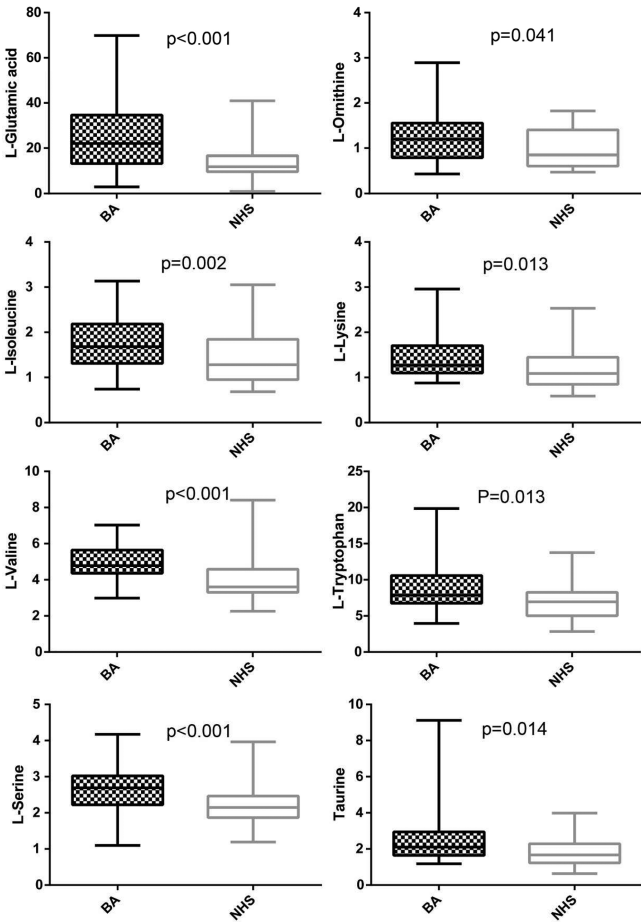


Figure 3. Differentially expressed amino acids and biogenic amines validated by UPLC-MS/MS between BA and NHS.

DISCUSSION

In this study, we systematically profiled total plasma metabolites in BA, NHS, and healthy infants using GC-TOFMS. The OPLS-DA models derived from the metabolomic analysis showed clear separation among BA, NHS, and healthy infants. After the IPA analysis of the differentially expressed metabolites, UPLC-MS/MS was performed to validate the differentially expressed amino acids between BA and NHS.

Here untargeted GC-TOFMS and targeted UPLC-MS/MS were combined to discover and validate the metabolomic differences between BA and NHS. Untargeted GC-TOFMS was used to measure as many features as possible with no bias, and targeted UPLC-MS/MS was used to verify the potential biomarkers in a more reliable and robust manner.¹⁸ The comparison showed that the two platforms used in this study were both of great reliability. All of the differentially expressed

amino acids discovered in GC–TOFMS were also found to be significantly altered using UPLC–MS/MS.

IPA analysis revealed that “Cellular Function and Maintenance, Hepatic System Development and Function, Neurological Disease” was the most significantly altered network between BA and NHS (Figure 2). This is reasonable as both BA and NHS have severe liver dysregulation. There were five amino acids (L-glutamic acid, L-ornithine, L-lysine, L-tryptophan, and L-serine) involved in this network. The perturbations in amino acid metabolism are very well established in liver diseases, although the particular amino acids and directions of change are very complex.^{19,20} The increased level of seven amino acids in the BA group as compared with the NHS group obtained in our study was in agreement with the reports that the serum levels of all amino acids were elevated under circumstances of fulminant hepatic necrosis.¹⁹ It was reported that aromatic amino acids (AAA, tyrosine, and phenylalanine), taurine, aspartate, threonine, serine, asparagine, methionine, ornithine, and histidine were significantly increased in partially hepatectomized rats (65% of liver was removed), while in carbon-tetrachloride-induced liver cirrhosis, increased levels of AAA, aspartate, asparagine, methionine, ornithine, and histidine and decreased levels of branched-chain amino acids (BCAA; i.e., valine, leucine, and isoleucine) were observed.¹⁹ L-Glutamic acid is the core metabolite in the network and the most significant differentially expressed amino acid between BA and NHS. Zhao et al. also found the higher expression of L-glutamic acid compared with NHS, while both were still lower than healthy controls.⁵ It has been found that the development of acute liver failure induced a significant reduction in L-glutamic acid levels in pig models.²¹ L-Glutamic acid was also reported as a protective regulator for deoxynivalenol-induced damage manifested as oxidative stress, intestinal injury, and signaling inhibition.²² We found L-tryptophan was significantly elevated in BA compared with NHS, while no significant differences of L-tyrosine and L-phenylalanine were observed between the two groups. L-Glutamine was found marginally lower in BA compared with NHS ($p = 0.075$, data not shown) in our study, which is in agreement with the findings by Zhao et al. that L-glutamine was reduced in BA compared with NHS, while both were higher than normal control.⁵

It is worth noting that two of the BCAAs, L-valine and L-isoleucine, were more highly expressed in BA than NHS. Their downstream metabolite, 2-hydroxy-3-methylbutyric acid, was significantly decreased. BCAAs are receiving great attention nowadays as their predictive role in the occurrence of type 2 diabetes.²³ BCAAs were significantly decreased in carbon-tetrachloride-induced liver cirrhosis, while significantly elevated in acute carbon tetrachloride induced injury and ischemic damage.¹⁹ A recent article by Holecck et al. on amino acid alterations in liver cirrhosis were reviewed in detail,²⁰ and the best-known alteration is the decrease in BACC.²⁴ Furthermore, BCAA supplementation reduces oxidative stress and prolongs survival in rats with advanced liver cirrhosis²⁵ and restores the innate immune responses.²⁶ Although etiology of BA is unclear, immune dysregulation plays important roles in pathogenesis of the disease.²⁷ BA will eventually progress to liver cirrhosis^{1,28} and the significantly higher expression of γ -glutamyltransferase levels possibly indicates worse hepatic damage in the BA group. The difference in amino acid metabolism may reflect the different causes of liver damages between BA and NHS.^{29,30}

CONCLUSIONS

This study suggests that plasma metabolic profiling has great potential in differentiating BA from NHS, and amino acid metabolism is significantly different between the two diseases.

ASSOCIATED CONTENT

Supporting Information

Table S1: List of compounds identified in the plasma samples using GC–TOFMS. The Supporting Information is available free of charge on the ACS Publications website at DOI: 10.1021/pr5b00125.

AUTHOR INFORMATION

Corresponding Authors

*W.C.: Tel/Fax: 86-21-65791316. E-mail: caiw1978@163.com.

*W.J.: Tel/Fax: 01-808-5645823. E-mail: wjia@cc.hawaii.edu.

Notes

The authors declare no competing financial interest.

ACKNOWLEDGMENTS

This study is supported by Shanghai Key Laboratory of Pediatric Gastroenterology and Nutrition (14DZ2272400), National Natural Science Youth Foundation of China (81300516), Natural Science Foundation of Shanghai (13ZR1434200), Doctoral Fund of Ministry of Education of China (20130073120013), and Medicine-Engineering Cross Research Funding of Shanghai Jiao Tong University (YG2012MS03).

REFERENCES

- (1) Hartley, J. L.; Davenport, M.; Kelly, D. A. Biliary atresia. *Lancet* **2009**, 374 (9702), 1704–1713.
- (2) Mieli-Vergani, G.; Vergani, D. Biliary atresia. *Semin. Immunopathol.* **2009**, 31 (3), 371–381.
- (3) Sira, M. M.; Taha, M.; Sira, A. M. Common misdiagnoses of biliary atresia. *Eur. J. Gastroenterol. Hepatol.* **2014**, 26 (11), 1300–1305.
- (4) Peng, S. S.; Hsu, W. M.; Chen, H. L.; Mo, Y. H. Using volume index and lateral hepatic angle to differentiate biliary atresia from TPN-associated cholestasis. *J. Pediatr. Gastroenterol. Nutr.* **2014**, 59 (3), 403–408.
- (5) Zhao, D.; Han, L.; He, Z.; Zhang, J.; Zhang, Y. Identification of the plasma metabolomics as early diagnostic markers between biliary atresia and neonatal hepatitis syndrome. *PLoS One* **2014**, 9 (1), e85694.
- (6) Ukarapol, N.; Wongsawadi, L.; Ong-Chai, S.; Riddhiputra, P.; Kongtawelert, P. Hyaluronic acid: additional biochemical marker in the diagnosis of biliary atresia. *Pediatr. Int.* **2007**, 49 (5), 608–611.
- (7) Song, Z.; Dong, R.; Fan, Y.; Zheng, S. Identification of serum protein biomarkers in biliary atresia by mass spectrometry and enzyme-linked immunosorbent assay. *J. Pediatr. Gastroenterol. Nutr.* **2012**, 55 (4), 370–375.
- (8) El-Faramawy, A. A.; El-Shazly, L. B.; Abbass, A. A.; Ismail, H. A. Serum IL-6 and IL-8 in infants with biliary atresia in comparison to intrahepatic cholestasis. *Trop. Gastroenterol.* **2011**, 32 (1), 50–55.
- (9) Zahm, A. M.; Hand, N. J.; Boateng, L. A.; Friedman, J. R. Circulating microRNA is a biomarker of biliary atresia. *J. Pediatr. Gastroenterol. Nutr.* **2012**, 55 (4), 366–369.
- (10) Chen, T.; Xie, G.; Wang, X.; Fan, J.; Qiu, Y.; Zheng, X.; Qi, X.; Cao, Y.; Su, M.; Wang, X.; Xu, L. X.; Yen, Y.; Liu, P.; Jia, W. Serum and urine metabolite profiling reveals potential biomarkers of human hepatocellular carcinoma. *Mol. Cell. Proteomics* **2011**, 10 (7), M110.004945.
- (11) Xuan, J.; Pan, G.; Qiu, Y.; Yang, L.; Su, M.; Liu, Y.; Chen, J.; Feng, G.; Fang, Y.; Jia, W.; Xing, Q.; He, L. Metabolomic profiling to

identify potential serum biomarkers for schizophrenia and risperidone action. *J. Proteome Res.* **2011**, *10* (12), 5433–5443.

(12) Chen, W. L.; Wang, J. H.; Zhao, A. H.; Xu, X.; Wang, Y. H.; Chen, T. L.; Li, J. M.; Mi, J. Q.; Zhu, Y. M.; Liu, Y. F.; Wang, Y. Y.; Jin, J.; Huang, H.; Wu, D. P.; Li, Y.; Yan, X. J.; Yan, J. S.; Li, J. Y.; Wang, S.; Huang, X. J.; Wang, B. S.; Chen, Z.; Chen, S. J.; Jia, W. A distinct glucose metabolism signature of acute myeloid leukemia with prognostic value. *Blood* **2014**, *124* (10), 1645–1654.

(13) Mathe, E. A.; Patterson, A. D.; Haznadar, M.; Manna, S. K.; Krausz, K. W.; Bowman, E. D.; Shields, P. G.; Idle, J. R.; Smith, P. B.; Anami, K.; Kazandjian, D. G.; Hatzakis, E.; Gonzalez, F. J.; Harris, C. C. Noninvasive urinary metabolomic profiling identifies diagnostic and prognostic markers in lung cancer. *Cancer Res.* **2014**, *74* (12), 3259–3270.

(14) Chi, Y.; Pei, L.; Chen, G.; Song, X.; Zhao, A.; Chen, T.; Su, M.; Zhang, Y.; Liu, J.; Ren, A.; Zheng, X.; Xie, G.; Jia, W. Metabonomic profiling of human placentas reveals different metabolic patterns among subtypes of neural tube defects. *J. Proteome Res.* **2014**, *13* (2), 934–945.

(15) Spratlin, J. L.; Serkova, N. J.; Eckhardt, S. G. Clinical applications of metabolomics in oncology: a review. *Clin. Cancer Res.* **2009**, *15* (2), 431–440.

(16) Qiu, Y.; Cai, G.; Su, M.; Chen, T.; Zheng, X.; Xu, Y.; Ni, Y.; Zhao, A.; Xu, L. X.; Cai, S.; Jia, W. Serum metabolite profiling of human colorectal cancer using GC–TOFMS and UPLC–QTOFMS. *J. Proteome Res.* **2009**, *8* (10), 4844–4850.

(17) Sun, L.; Li, J.; Zhou, K.; Zhang, M.; Yang, J.; Li, Y.; Ji, B.; Zhang, Z.; Zhu, H.; Yang, L.; He, G.; Gao, L.; Wei, Z.; Wang, K.; Han, X.; Liu, W.; Tan, L.; Yu, Y.; He, L.; Wan, C. Metabolomic analysis reveals metabolic disturbance in the cortex and hippocampus of subchronic MK-801 treated rats. *PLoS One* **2013**, *8* (4), e60598.

(18) Zhu, J.; Djukovic, D.; Deng, L.; Gu, H.; Himmatti, F.; Chiorean, E. G.; Raftery, D. Colorectal cancer detection using targeted serum metabolic profiling. *J. Proteome Res.* **2014**, *13* (9), 4120–4130.

(19) Holecek, M.; Mraz, J.; Tilser, I. Plasma amino acids in four models of experimental liver injury in rats. *Amino Acids* **1996**, *10* (3), 229–241.

(20) Holecek, M. Ammonia and amino acid profiles in liver cirrhosis: effects of variables leading to hepatic encephalopathy. *Nutrition* **2015**, *31* (1), 14–20.

(21) Ytrebo, L. M.; Sen, S.; Rose, C.; Ten Have, G. A.; Davies, N. A.; Hodges, S.; Nedredal, G. I.; Romero-Gomez, M.; Williams, R.; Revhaug, A.; Jalan, R.; Deutz, N. E. Interorgan ammonia, glutamate, and glutamine trafficking in pigs with acute liver failure. *American journal of physiology. Am. J. Physiol.: Gastrointest. Liver Physiol.* **2006**, *291* (3), G373–G381.

(22) Wu, M.; Xiao, H.; Ren, W.; Yin, J.; Tan, B.; Liu, G.; Li, L.; Nyachoti, C. M.; Xiong, X.; Wu, G. Therapeutic effects of glutamic acid in piglets challenged with deoxynivalenol. *PLoS One* **2014**, *9* (7), e100591.

(23) Wang, T. J.; Larson, M. G.; Vasan, R. S.; Cheng, S.; Rhee, E. P.; McCabe, E.; Lewis, G. D.; Fox, C. S.; Jacques, P. F.; Fernandez, C.; O'Donnell, C. J.; Carr, S. A.; Mootha, V. K.; Florez, J. C.; Souza, A.; Melander, O.; Clish, C. B.; Gerszten, R. E. Metabolite profiles and the risk of developing diabetes. *Nat. Med.* **2011**, *17* (4), 448–453.

(24) Morgan, M. Y.; Marshall, A. W.; Milsom, J. P.; Sherlock, S. Plasma amino-acid patterns in liver disease. *Gut* **1982**, *23* (5), 362–370.

(25) Iwasa, M.; Kobayashi, Y.; Mifuji-Moroka, R.; Hara, N.; Miyachi, H.; Sugimoto, R.; Tanaka, H.; Fujita, N.; Gabazza, E. C.; Takei, Y. Branched-chain amino acid supplementation reduces oxidative stress and prolongs survival in rats with advanced liver cirrhosis. *PLoS One* **2013**, *8* (7), e70309.

(26) Nakamura, I.; Ochiai, K.; Imai, Y.; Moriyasu, F.; Imawari, M. Restoration of innate host defense responses by oral supplementation of branched-chain amino acids in decompensated cirrhotic patients. *Hepatol. Res.* **2007**, *37* (12), 1062–1067.

(27) Feldman, A. G.; Mack, C. L. Biliary atresia: cellular dynamics and immune dysregulation. *Semin. Pediatr. Surg.* **2012**, *21* (3), 192–200 3399127.

(28) Diniz, G.; Tosun Yildirim, H.; Calkavur, S.; Ecevit, C.; Olukman, O.; Bekem Soylu, O.; Aktas, S. Can Neonatal Hepatitis Be More Fatal than Biliary Atresia? *Fetal Pediatr. Pathol.* **2015**, DOI: 10.3109/15513815.2014.999393.

(29) Rastogi, A.; Krishnani, N.; Yachha, S. K.; Khanna, V.; Poddar, U.; Lal, R. Histopathological features and accuracy for diagnosing biliary atresia by prelaparotomy liver biopsy in developing countries. *J. Gastroenterol. Hepatol.* **2009**, *24* (1), 97–102.

(30) El-Guindi, M. A.; Sira, M. M.; Sira, A. M.; Salem, T. A.; El-Abd, O. L.; Konsowa, H. A.; El-Azab, D. S.; Allam, A. A. Design and validation of a diagnostic score for biliary atresia. *J. Hepatol.* **2014**, *61* (1), 116–123.